



ELSEVIER

Superlattices and Microstructures 36 (2004) 763–772

Superlattices
and Microstructures

www.elsevier.com/locate/superlattices

Optical properties of InGaN quantum dots

M. Dworzak*, T. Bartel, M. Straßburg¹, I.L. Krestnikov,
A. Hoffmann, R. Seguin, S. Rodt, A. Strittmatter, D. Bimberg

Institut für Festkörperphysik, Technische Universität Berlin, Hardenbergstraße 36, 10623 Berlin, Germany

Available online 12 October 2004

Abstract

We present time-resolved and spatially-resolved photoluminescence (PL) measurements of InGaN inclusions in a GaN matrix. The structures were grown by metal-organic chemical vapor deposition on sapphire and Si(111) substrates. Nonresonant pulsed excitation yields a broad PL peak, while resonant excitation into the nonresonant PL intensity maximum results in an evolution of a sharp resonant PL peak, having a spectral shape defined by the excitation laser pulse and a radiative decay time close to that revealed for PL under nonresonant excitation. Observation of a resonantly excited narrow PL line gives clear proof of the quantum dot (QD) nature of luminescence in InGaN–GaN samples. Cathodoluminescence (CL) and micro-PL measurements demonstrate sharp emission lines from single QD states. The recombination dynamics of single QD's and the whole QD ensemble were investigated. Monoexponential decay was observed for the PL of single QD's. For similar transition energies different time constants were obtained. Therefore the nonexponential decay observed for the whole ensemble is attributed to the coexistence of QD's having similar ground-state transition energies, but significantly different electron–hole overlap.

© 2004 Elsevier Ltd. All rights reserved.

Group III nitride-based optoelectronic devices are used in a wide range of applications due to their large band gap energies. InGaN/GaN heterostructures form the active layer in blue–green LED's and laser diodes commercially available today [1]. Quantum dot (QD)

* Corresponding author. Tel.: +49 30 314 24440; fax: +49 30 22064.

E-mail address: dworzak@physik.tu-berlin.de (M. Dworzak).

¹ Present address: Department of Physics and Astronomy, Georgia State University, Atlanta, GA-30303, USA.

structures could still improve their performance enormously [2]. In particular, InGaN QD lasers are expected to have low threshold current densities and better temperature stability compared with conventional blue lasers with InGaN quantum wells (QW) [3]. Some researchers [4–6] proposed that indium fluctuations in ultra-thin InGaN layers represent ultra dense (10^{11} cm^{-2}) arrays of QD's. These QD's are found to be responsible for good luminescence properties of thin InGaN layers [7], as they suppress carrier diffusion towards various defects and were claimed to be crucial for lasing in InGaN-based injection structures [8]. Previously, we emphasized that the maximum modal gain is directly proportional to the volume density of QD's [9], and a maximum modal gain of about 10^5 cm^{-1} may be realized for wide-gap QD's having a density of 10^{18} cm^{-3} and a density-of-states broadening of a few tens of meV [2,5]. This opens unique possibilities for device applications, particularly, for lasers. Consequently, InGaN QD structures have been intensively investigated in recent time. Growth of nanometer-scaled islands, similar to the well-known Stranski–Krastanov growth mode, as well as QD properties of In-rich fluctuations were reported [3,10–13]. Spatially resolved luminescence experiments demonstrated sharp emission lines originating from single QD states with δ -like density of states [13,14]. Time-resolved luminescence investigations on such emission lines were reported [14]. Nevertheless, the QD nature of ultra-thin InGaN-layers is still under controversial discussion. Many groups reported a long-wavelength shift of the InGaN PL after pulsed excitation accompanied by a significant increase in the PL decay time [15–18]. Additionally a blueshift of the PL with increasing continuous-wave excitation density was observed [19]. In both cases, screening of piezoelectric fields separating electrons and holes in a QW at high excitation densities was proposed to be responsible for the above effects. In a QD no further population is possible in the case of a photon having exactly the same energy, after the first exciton is created in a QD. Thus, no screening of piezoelectric fields with increased excitation density is possible. This is opposite to the QW case, where a continuum of states exists, and a lot of electron–hole pairs can be created in the same QW.

In this report we present time-resolved and spatially resolved photoluminescence (PL) as well as cathodoluminescence (CL) investigations on InGaN structures that unambiguously evidence the QD origin of the InGaN luminescence. Monoexponential decay of the PL is found for emission lines from single QD's. Meanwhile a nonexponential decay was observed for the luminescence of the entire QD ensemble. This behavior is attributed to disorder in the size and in the composition distribution of the QD's. Furthermore, the spectral dependence of the QD ensemble PL decay shows the relevance of transfer processes.

Sample A, grown on a (0001) *c*-plane sapphire substrate by metal-organic chemical vapor deposition (MOCVD), consists of a 2.5 μm GaN buffer layer, with an active region of a 10-period InGaN/GaN superlattice and a 0.07 μm GaN cap layer, formation of a 3 nm InGaN/7 nm GaN superlattice was achieved by periodic substrate temperature variation from 820 to 915 $^{\circ}\text{C}$. Sample B was grown by low-pressure MOCVD on Si(111) surface. An AlN layer acting as nucleation surface was obtained by using a previously described conversion process of AlAs to AlN [20]. In the following step $\text{Al}_{0.05}\text{Ga}_{0.95}\text{N}$ /GaN buffer layers were grown at $T = 1150 \text{ }^{\circ}\text{C}$ up to a total thickness of 1 μm . The InGaN layers were grown at 800 $^{\circ}\text{C}$. Total pressure was kept at 400 mbar during InGaN deposition. The growth was finished with a 20 nm GaN cap layer grown during heatup to 1100 $^{\circ}\text{C}$.

Sample B was masked with a 70 nm thick metal cap leaving apertures of 100 and 200 nm diameter for spatially resolved investigations. Previous cross section TEM measurements on both samples showed composition fluctuations in the InGaN layer with indium rich domains. Their lateral size of about 5 nm is comparable to the exciton Bohr radius, thus small enough to provide for strong localization of excitons and confinement of their wave functions [13].

Sample A was investigated by time-resolved PL spectroscopy at 2 K under tunable dye laser excitation with a repetition rate of 3.79 MHz at wavelengths of 291 nm (4.26 eV) and 424 nm (2.925 eV). Sample B was investigated by time-resolved and spatially-resolved PL and CL spectroscopy. The PL was excited at 353 nm (3.51 eV) by the second harmonic wave of a mode-locked Ti:sapphire laser. The temporal width of the laser pulses was 2 ps at a repetition rate of 80 MHz. The PL measurements were performed in a helium-flow microscope cryostat at a temperature of 5 K. The luminescence light was collected through a microscope objective. While the luminescence of the entire QD ensemble was detected from unmasked areas single QD luminescence was detected through 200 nm apertures in the metal mask. The detection system for all PL measurements consisted of two 0.35 m McPherson monochromators in subtractive mode and an ultra-fast photo detector (micro-channel plate) providing a spectral resolution of about 1 meV and a time resolution of better than 30 ps. CL measurements were performed with a JEOL JSM 840 scanning electron microscope equipped with a cathodoluminescence setup. All CL measurements were made at a temperature of 6.5 K. The luminescence light was dispersed by a 0.3 m monochromator equipped with a 2400 lines/mm grating and detected with a nitrogen cooled Si-CCD camera, providing a spectral resolution of 310 μ eV at 3 eV.

In Fig. 1 the temporal evolution of the PL intensity for both samples is shown. The rise time was found below the detection limit. A nonexponential decay was observed. This behavior is typical for heavily disordered materials and is fitted by the stretched exponential model [21]

$$I(t) = I_0 \exp[-(t/\tau^*)^\beta] \quad (1)$$

(solid lines in Fig. 1(a) and (b)). Here, τ^* is the time constant and β is the stretching parameter. The variation of β from unity is a measure for the degree of disorder in the material. Values from 0.35 to 0.80 were obtained. This well-known nonexponential behavior [11, 12, 14] was previously interpreted as a temporal dependence of the decay time. It was attributed to the screening of piezoelectric fields which influences electron–hole wave-function overlap through the Quantum-Confined Stark-Effect (QCSE). It was suggested that at high excitation densities, reached by pulsed lasers, piezoelectric fields could be screened by nonequilibrium charge carriers. This screening would initially lead to a stronger wave-function overlap, while progressive depopulation would be followed by electron–hole separation and result in increasing life times [22]. This effect should be dependent on excitation density. We observed that a decrease of the excitation density of two orders of magnitude did not result in any change of the shape or the time constant of the transient PL. Thus the screening of piezoelectric fields cannot be responsible for the nonexponential PL decay.

Morel et al. [11] offer an alternative explanation that can be related to a broad distribution of exciton life times in localization centers with similar transition energies.

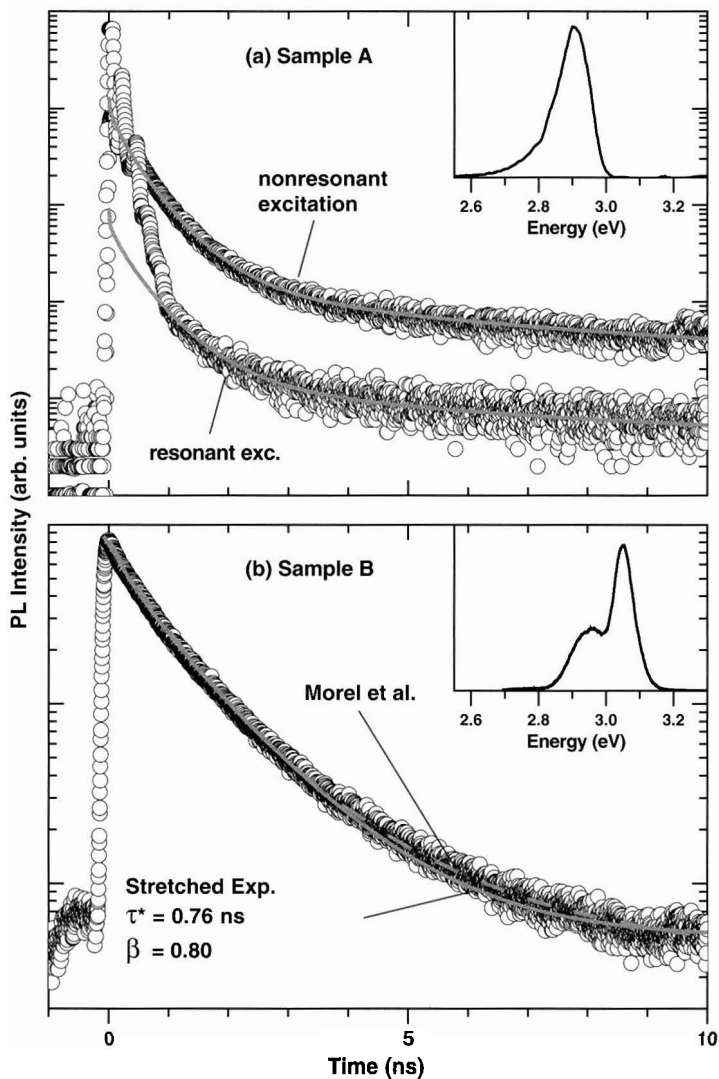


Fig. 1. Time-resolved PL, fits with Eq. (1) (solid lines) and after Morel et al. (dashed line in Fig. 1(b)), inset: time-integrated PL.

They attribute the variation of life times to an in-plane separation of electrons and holes. A ‘Pseudo-DAP’ model based on Thomas et al. [23] is developed for the recombination dynamic. The recombination probability depends on the lateral distance r between electron and hole:

$$W(r) = W_{\max} e^{-r^2/a^2}, \quad (2)$$

where a denotes the characteristic distance of the localization centers. The time dependence of the luminescence intensity is given by

$$I(t) = \left\{ 2\pi n \int_0^\infty W(r) \exp[-W(r)t] r dr \right\} \times \left\{ \exp \left[2\pi n \int_0^\infty (\exp[-W(r)t] - 1) r dr \right] \right\}. \quad (3)$$

While W_{\max} calibrates the time axis $\eta = n \cdot a^2$ defines the shape of the decay function. Since n denotes the density of localization centers, η characterizes the degree of localization. Though this model yields a good approximation of our results (dashed line in Fig. 1(b)), it will be shown that individual QD's have different exciton life-times and that this leads to the nonexponential decay of the QD ensemble.

One experiment, which can clarify unambiguously the nature of the processes involved, is the resonant excitation of the time-resolved PL. In Fig. 2 we present the PL of sample A in a time/wavelength plot. The excitation wavelength exactly matches the PL maximum. After the excitation pulse (white color) the shape of the PL spectrum is completely different to the nonresonant case. Most of the PL intensity exactly resembles the spectral shape of the excitation source. Even the nonexponential decay of this signal corresponds to the PL decay after nonresonant excitation (see Fig. 1(a)). This unambiguously evidences the QD origin of the sample. The PL peak does not shift in time and no spectral broadening was observed. This may additionally rule out any importance of the gradual weakening of the piezoelectric screening with carrier depopulation, that takes place in QW samples. The observed behavior fits exactly the behavior of resonantly excited QD's having a delta-function-like density of states [12].

Spatially high-resolved CL measurements show discrete QD states in our structures and demonstrate 3-D confinement of carriers in InGaN QD's [13]. When detected through one aperture of the shadow mask the broad luminescence peak of the QD ensemble decomposes into sharp lines (Fig. 3). The narrowest observed line shows a full width at half maximum (FWHM) of 0.48 meV. These lines were observed from 2.8 to 3.2 eV indicating QD origin of the entire broad peak. Time series of single line spectra with short integration time (80–300 ms) show slight stochastic variations of the peak energies and intensities due to fluctuating electric fields. The source of these fields is charging and discharging of nearby defects or interface states [24,25]. This effect can be used to correlate transitions that originate from the same QD, since they experience the same electric fields, and hence, the lines exhibit the same energetic jitter and intensity behavior [26]. Doublets and triplets showing a similar jitter could be observed [13]. The presence of such groups demonstrate the existence of higher excitonic complexes in one QD. Linear and quadratic dependence on the excitation density were found. This behavior is typical for excitons and biexcitons [27].

Time-resolved PL measurements on the observed single QD lines as well as on the entire QD ensemble were performed. In Fig. 4 the spectral dependence of the PL time constants for sample B is shown. The fitting parameter τ^* from the stretched exponential and the $1/e$ decay time τ_e are presented. Both time constants show a similar spectral dependence. Their decrease with increasing energies is generated by the rise of transfer processes

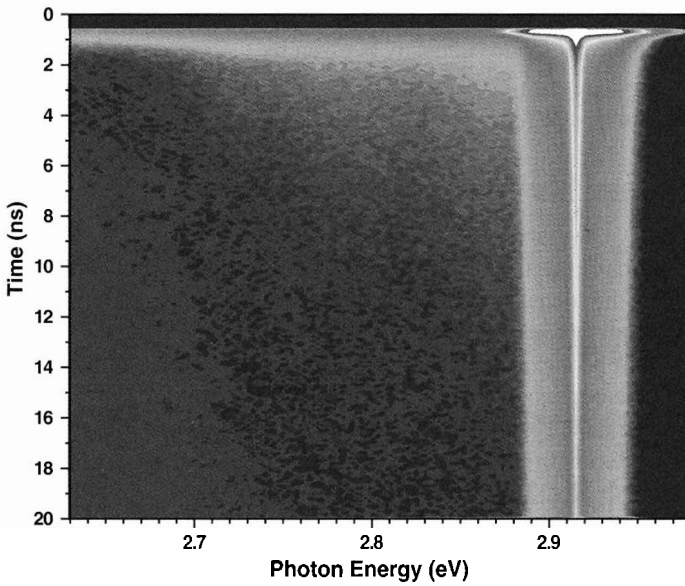


Fig. 2. Time/wavelength plot for resonant excitation (sample A). White spot corresponds to the scattered laser light.

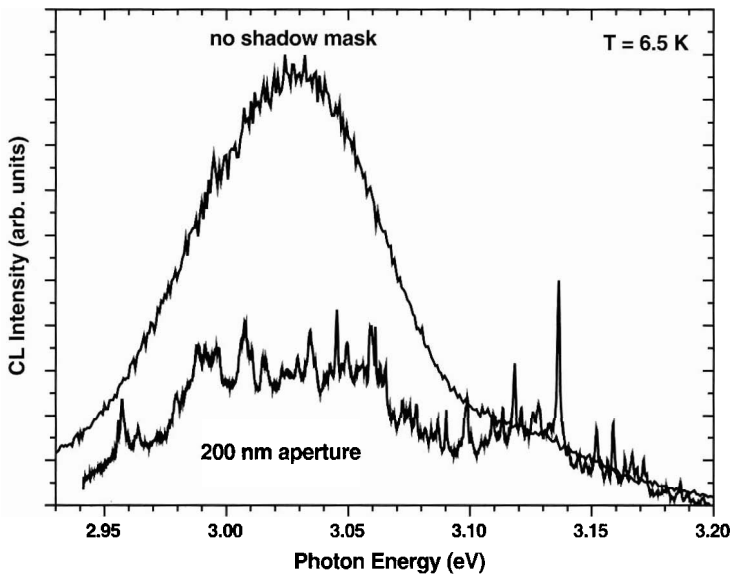


Fig. 3. CL of sample B without shadow mask and through a 200 nm aperture.

from QD's providing smaller localization energy. Hence, the decrease of the decay time with increasing energies indicates the rising contribution of nonradiative recombination

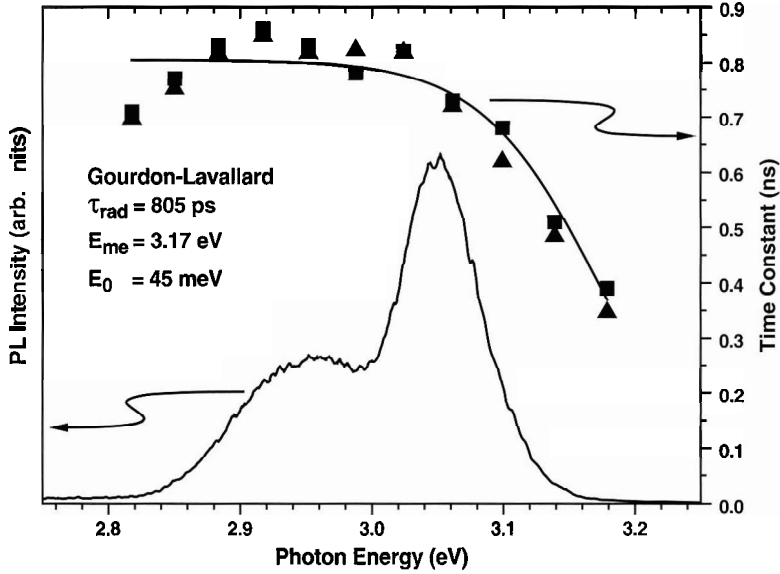


Fig. 4. Time-integrated ensemble PL of sample B, time constant τ_e of the $1/e$ -decay (squares) and the fitting parameter τ^* (triangles), fit with Eq. (4) (solid line).

of localized excitons. To determine the radiative lifetime of the localized excitons as well as their average binding energy and mobility properties, we evaluated the results with a model introduced by Gourdon and Lavallard [28] accounting for lateral energy transfer in a high-density QD ensemble [29]. Assuming the density of tail states is proportional to $\exp(-E/E_0)$ the PL decay time for excitons in localized states as a function of the spectral position can be described by:

$$\tau(E) = \frac{\tau_{rad}}{1 + \exp[(E - E_{me})/E_0]}, \quad (4)$$

where τ_{rad} is the radiative lifetime, E_{me} the energy for which the radiative lifetime equals the lateral transfer time and E_0 is a characteristic energy for the density of states. The latter parameter is a measure for the average localization energy of the QD's. E_{me} denotes the change from 3-D-localized QD states to QW states with higher exciton mobility. Above this energy the transfer of excitons is more probable than their radiative decay. Applying Eq. (4) (solid line in Fig. 1(a)) yields a radiative lifetime of $\tau_{rad} \sim 805$ ps, an average binding energy of $E_0 \sim 45$ meV and an $E_{me} \sim 3.17$ eV. The most striking result is that nearly the whole PL is emitted at energies below E_{me} . Thus, the spectral dependence of τ^* and τ_e yields another unambiguous proof for the QD origin of the luminescence. While Eq. (4) gives a good approximation for our results at higher energies, both, τ^* and τ_e differ from the fitting curve on the low energy tail of the QD ensemble emission band. We attribute the decrease of the decay times with lower energy to an increasing confinement of excitons in QD's with higher localization energy and thus with a higher electron-hole overlap.

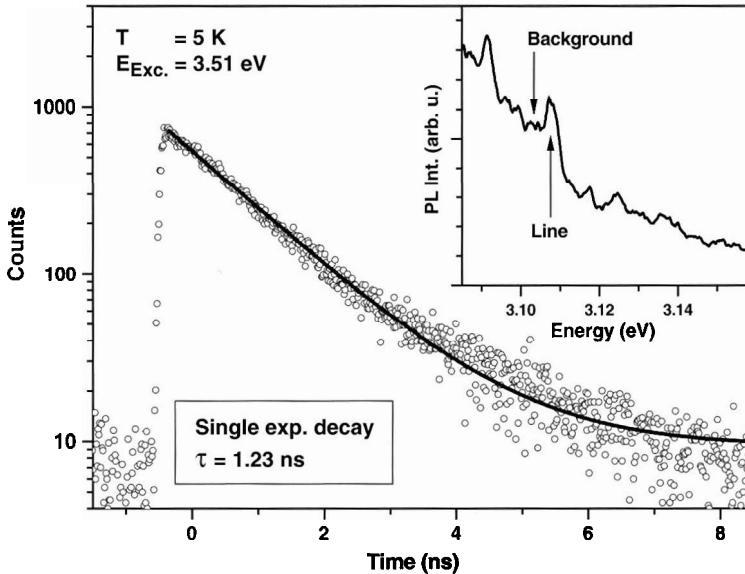


Fig. 5. Time-resolved PL of a single QD emission line (inset), fitted by a monoexponential decay (solid line).

The dynamics of excitons in single QD's were investigated using μ -PL. Fig. 5 shows the transient behavior of a single QD line emphasized in the inset. Superimposed to the studied line there is a background signal that made up to 70% of the PL intensity. This background signal is attributed to luminescence light from the QD ensemble transmitted through the mask and scattered light from other mask holes. To eliminate the transient behavior of the background and isolate the single QD emission line two transients for each QD line were recorded: one detected at the maximum of the line and one 5–10 meV aside. Since the changes in the PL dynamic of the entire QD ensemble are negligible for energy differences of a few meV, the latter transient was subtracted from the first to obtain the true PL decay of the single QD state as suggested by Robinson et al. [14]. As opposed to the ensemble luminescence single QD lines show a single-exponential behavior. Their decay times range between 0.4 and 1.6 ns.

In Fig. 6 the observed decay times as a function of the transition energy are depicted for the ensemble luminescence (squares) and for the investigated single QD's (triangles). A large spread of the latter was observed even at similar detection energies. Consequently, QD states with the same transition energy do not necessarily have the same exciton lifetime. In fact, the dynamics of luminescence are governed by two competing processes: the transition probability which primarily depends on electron–hole wave-function overlap and the probability of nonradiative escape. The wave-function overlap is affected by QD size, shape and the depth of its localizing potential. The latter is not given by its absolute indium content, but depends on the difference of the indium concentration in the QD and its adjacent area. Due to the disordered distribution of the indium content in the investigated sample [13], there is no correlation of the localization energy to the transition energy. Luminescence at a certain detection energy originates from a QD sub-ensemble

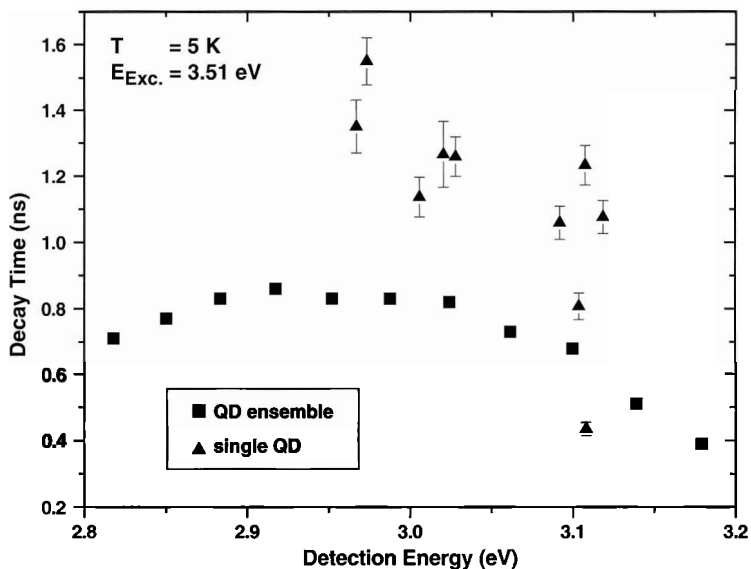


Fig. 6. Spectral dependence of time constants for single QD lines (triangles) and the QD ensemble (squares).

with the same transition energy. However, this sub-ensemble still consists of QD's with a broad distribution of electron-hole wave-function overlap. The transfer probability shows a similar behavior. Generally, the trend towards shorter time constants for higher transition energies (Fig. 6) can be explained by an increasing importance of escape processes. Nevertheless, the transfer probability also differs inside one QD sub-ensemble. For QD's of a sub-ensemble this leads to different time constants. Thus the nonexponential PL decay is assigned to the summation of monoexponential decays originating from individual QD's.

In conclusion, observation of a resonantly excited narrow PL line and sharp CL lines originating from single QD states gives clear proof of the QD nature of luminescence in our InGaN samples. In addition, the recombination dynamics of excitons localized in a single InGaN QD was compared to the recombination dynamics of the entire QD ensemble. The dynamic of the exciton decay was found to be monoexponential. The nonexponential PL decay of the entire QD ensemble gives an unambiguous proof that the disorder of the QD system governs the recombination dynamics.

Acknowledgements

The authors acknowledge I.P. Soshnikov, A.F. Tsatsul'nikov and W.V. Lundin from the A.F. Ioffe Physical-Technical Institute, St. Petersburg, Russia, for the preparation of the sample grown on sapphire. This work was supported by the Deutsche Forschungsgemeinschaft in the framework of SFB296. M. Straßburg and I.L. Krestnikov gratefully acknowledge the support by the Alexander von Humboldt Foundation.

References

- [1] S. Nakamura, G. Fasol, *The Blue Laser Diode*, Springer, Berlin, 1997.
- [2] e.g., D. Bimberg, M. Grundmann, N.N. Ledentsov, *Quantum Dot Heterostructures*, Wiley, New York, 1999.
- [3] Y. Arakawa, *IEEE J. Sel. Top. Quantum Electron.* 8 (2002) 823.
- [4] S. Chichibu, T. Azuhata, T. Sota, S. Nakamura, *Appl. Phys. Lett.* 69 (1996) 4188.
- [5] N.N. Ledentsov, Zh.I. Alfvov, I.L. Krestnikov, W.V. Lundin, A.V. Sakharov, I.P. Soshnikov, A.F. Tsatsul'nikov, D. Bimberg, A. Hoffmann, *Comp. Semicond.* 5 (9) (1999) 61.
- [6] A.V. Sakharov, W.V. Lundin, I.L. Krestnikov, V.A. Semenov, A.S. Usikov, A.F. Tsatsul'nikov, yu.G. Musikhin, M.V. Baidakova, Zh.I. Alfvov, N.N. Ledentsov, J. Holst, A. Hoffmann, D. Bimberg, I.P. Soshnikov, D. Gerthsen, *Phys. Status Solidi b* 216 (1999) 435.
- [7] K.P. O'Donnell, R.W. Martin, P.G. Middleton, *Phys. Rev. Lett.* 82 (1999) 237.
- [8] Y. Narukawa, Y. Kawakami, M. Funato, S. Fujita, S. Fujita, S. Nakamura, *Appl. Phys. Lett.* 70 (1997) 981.
- [9] M. Asada, M. Miyamoto, Y. Suematsu, *IEEE J. Quantum Electron.* QE-22 (1986) 1915.
- [10] B. Damilano, N. Grandjean, S. Dalmaso, J. Massies, *Appl. Phys. Lett.* 75 (1999) 3751.
- [11] A. Morel, P. Lefebvre, T. Taliercio, T. Bretagnon, B. Gil, N. Grandjean, B. Damilano, J. Massies, *Physica E* 17 (2003) 64.
- [12] I.L. Krestnikov, N.N. Ledentsov, A. Hoffmann, D. Bimberg, A.V. Sakharov, W.V. Lundin, A.F. Tsatsul'nikov, A.S. Usikov, Z.I. Alferov, Y.G. Musikhin, D. Gerthsen, *Phys. Rev. B* 66 (2002) 155310.
- [13] R. Seguin, S. Rodt, A. Strittmatter, T. Bartel, A. Hoffmann, D. Bimberg, E. Hahn, D. Gerthsen, *Appl. Phys. Lett.* 84 (2004) 4023.
- [14] J.W. Robinson, J.H. Rice, A. Jarjour, J.D. Smith, R.A. Oliver, G.A.D. Briggs, M.J. Kappers, C.J. Humphreys, Y. Arakawa, *Appl. Phys. Lett.* 83 (2003) 2674.
- [15] H. Yu, H. Htoon, A. deLozanne, C.K. Shih, P.A. Grudowski, R.D. Dupuis, K. Zeng, R. Mair, J.Y. Lin, H.X. Jiang, *J. Vac. Sci. Technol. B* 16 (1998) 2215.
- [16] H. Kudo, H. Ishibashi, R. Zheng, Y. Yamada, T. Taguchi, *Appl. Phys. Lett.* 76 (2000) 1546.
- [17] S. Chichibu, T. Azuhata, T. Sota, S. Nakamura, *Appl. Phys. Lett.* 69 (1996) 4188.
- [18] J. Li, K.B. Nam, K.H. Kim, J.Y. Lin, H.X. Jiang, *Appl. Phys. Lett.* 78 (2001) 61.
- [19] T. Takeuchi, Sh. Sota, M. Katsuragawa, M. Komori, H. Takeuchi, H. Amano, I. Akasaki, *Japan. J. Appl. Phys. Part 2* 36 (1997) L382.
- [20] A. Strittmatter, A. Krost, M. Strasburg, V. Türk, D. Bimberg, J. Bläsing, J. Christen, *Appl. Phys. Lett.* 74 (1999) 1242.
- [21] H. Scher, M.F. Shlesinger, J.T. Bender, *Phys. Today* 26 (1991) 24.
- [22] M. Pophristic, F.H. Long, C. Tran, I.T. Ferguson, R.F. Karlicek, *Appl. Phys. Lett.* 76 (1999) 1114.
- [23] D.G. Thomas, J.J. Hopfield, W.M. Augustiniak, *Phys. Rev.* 140 (1965) A202.
- [24] S.A. Empedocles, D.J. Norris, M.G. Bawendi, *Phys. Rev. B* 77 (1996) 3873.
- [25] P. Castrillo, D. Hessman, M.-E. Pistol, J.A. Prieto, *Japan. J. Appl. Phys.* 36 (1997) 4188.
- [26] V. Türk, S. Rodt, O. Stier, R. Heitz, R. Engelhardt, U.W. Pohl, D. Bimberg, *Phys. Rev. B* 61 (2000) 9944.
- [27] M. Grundmann, D. Bimberg, *Phys. Rev. B* 55 (1997) 9740.
- [28] C. Gourdon, P. Lavallard, *Phys. Status Solidi b* 153 (1989) 641.
- [29] M. Straßburg, M. Dworzak, H. Born, R. Heitz, A. Hoffmann, M. Bartels, K. Lischka, D. Schikora, J. Christen, *Appl. Phys. Lett.* 80 (2002) 473.